Journal of
Materials Chemistry B

Accepted Manuscript

This article can be cited before page numbers have been issued, to do this please use: A. A. Mohammed, J. Aviles Milan, S. Li, J. J. Chung, M. M. Stevens, T. K. Georgiou and J. R. Jones, *J. Mater. Chem. B*, 2019, DOI: 10.1039/C9TB00658C.

ROYAL SOCIETY OF CHEMISTRY

rsc.li/materials-b

DOI: 10.1039/C9TB00658C

Open vessel free radical photopolymerization of double network gels for biomaterial applications using glucose oxidase

Ali A. Mohammed, † Juan Aviles Milan, † Siwei Li, † Justin J. Chung, † Molly M. Stevens, †,‡,§ Theoni K. Georgiou, † Julian R. Jones †,*

† Department of Materials, Imperial College London, SW7 2AZ, London, UK

‡ Institute of Biomedical Engineering, Imperial College London, SW7 2AZ, London, UK

§ Department of Bioengineering, Imperial College London, SW7 2AZ, London, UK

Abstract

Polymerization of certain gels in the presence of oxygen can lead to hindered reaction rates and low conversion rates, limiting the use of open vessel polymerization and material synthesis. Here, the oxido-reductase enzyme glucose oxidase (GOx) was used to enable open vessel free radical photopolymerization (FRP) of neutral polyacrylamide (PAAm), and polyelectrolyte poly (2-acrylamido-2-methyl-1-propanesulfonic acid) (PAMPS) under ambient conditions. GOx successfully blocks the inhibition pathways created by O_2 in FRP, dramatically increasing the polymer conversion rate for both polymers. In the presence of GOx, PAAm and PAMPS achieved conversion of 78 % and 100 % respectively at a photoinitiator (PI) concentration of 0.05 wt % with GOx, compared to 0 % without GOx at the same PI concentration. Cytotoxicity studies of these polymers show high cell viability after GOx is denatured. Double network hydrogels (DNHGs) were successfully produced using the polymers and use of GOx improved compressive fracture stress by a factor of ten. Vinyl functionalized silica nanoparticles (VSNPs) were used as cross linkers of the first network to further enhance the mechanical properties.

View Article Online
DOI: 10.1039/C9TB00658C

Keywords

Open vessel photopolymerization, photoinitiator, glucose oxidase, oxygen inhibition, free radical polymerization, hydrogels

Introduction

Polymeric biomaterials are often synthesized by different methods of free radical polymerization (FRP) for medical applications such as tissue engineering scaffolds, drug delivery systems or regenerative tissue replacements.[1-4] A popular type of FRP is photopolymerization. UV light curing is commonly used for its low cost, speed and ease of use, to prepare biocompatible materials such as hydrogels for cartilage repair applications.[1]

Double network hydrogels (DNHG) utilize contrasting properties of two separate polymers to create a synergistic properties.[5] They were developed by Gong[6] and have the ability to hold high water content while maintaining mechanical strength and toughness. Polyacrylamide (PAAm) and poly(2-acrylamido-2-methyl-1-propanesulfonic acid) (PAMPS) have successfully been used to create DNHGs through two-step sequential photopolymerizations.[5] DNHGs containing 90 wt% water showed improved stiffness (elastic modulus 1.0 – 1.0 MPa), strength (tensile failure stress of 10 MPa at 2000 % strain, compressive failure stress of 60 MPa, at 95 % strain) and toughness (tearing fracture energy 4400 $J.m^{-2}$) compared to single network gels and interpenetrating networks (simultaneous in situ polymerisation) of the same polymers.[5, 7-9] The DNHG synthesis was performed under closed nitrogen or argon purged systems, to avoid the presence of oxygen, but the apparatus limits the size and shape of the material due to practical aspects of purging.

The properties of these materials are affected by the presence of oxygen during synthesis as oxygen inhibits the free radicals that initiate the polymerization. Scheme 1 outlines the possible pathways which O_2 can inhibit FRP, labelled i1, i2 and i3, plus their corresponding O_2 evasion pathways e1, e2 and e3. [10-13] Pathway i1 highly depends on the efficiency and speed at which photoinitiators (PI) react. If the PI speed is fast enough, O_2 scavenging cannot compete.[14] This pathway is also affected by factors such as O_2 concentration in the media, the type (organic, inorganic) and viscosity of the media and the rate constant of bimolecular quenching of the

triplet state.[14] As a consequence of i1, initiating radicals created by photolysis are scavenged, leading to the inhibition of radical polymerization. i1 can be evaded as expressed in e1 – e3 by increasing PI concentration or increasing UV light intensity. However, O_2 would still be detrimental to the polymer kinetics and final conversion due to pathways i2 and i3. The combination of these inhibition pathways increases the induction time, resulting in a slower kinetic profile and yielding a low conversion ratio.[14] Propagating microradicals are converted to highly stable peroxy radicals that don't participate in, and can potentially hinder, photopolymerization.[15] Ultimately, the net efficiency of FRP is significantly altered leading to non-homogenous, sticky and wet polymer solutions, slower kinetics and low conversions. Therefore, creating an oxygen free environment is essential in restoring the efficiency of polymerization.[16, 17]

Other methods of O_2 elimination, other than nitrogen or argon purging, include paraffin waxes that act as O_2 barriers;[12, 14] the addition of O_2 scavengers,[18] such as thiols, phosphines and acrylic amines;[19-21] and the addition of surface active photoinitiators.[22] It is also possible to overwhelm O_2 by increasing PI concentration so that the free radical species outnumber the O_2 molecules, and by increasing the intensity of the UV light.[16] Increasing the PI concentration can cause cytotoxicity if the material is used in biomedical applications. These methods, despite their somewhat successful rates of O_2 evasion, require further cost and design to facilitate their use.

Here, the aim was to produce PAAm and PAMPS through FRP in an open-air system that would allow facile production of double network gels. The polymerization should occur with superior kinetics and conversion ratios under lower photoinitiator concentrations than the methods described above, at lower cost. A naturally occurring oxido-reductase enzyme, glucose oxidase (GOx), previously aided complete removal of O_2 in an open vessel system for reversible addition-fragmentation chain-transfer (RAFT) polymerization of hydroxyethyl acrylate and

dimethylacrylamide.[23] GOx reacts with glucose in the presence of O_2 to generate soluble by-products hydrogen peroxide and D-glucono- δ -lactone that are non-cytotoxic at low concentrations. This reaction was shown to be effective in in a variety of solvents such as phosphate buffered saline (PBS), water (pH range of 6-7), *tert*-butanol, acetonitrile and dioxane.[23] as low concentrations of GOx (200 nM) and glucose (100 nM) completely removed O_2 from an entire open vessel system, allowing reactions to occur.[23, 24] Here, an objective was to apply this process to FRP of PAMPS and PAAm for DNHGs.

Developing DNHGs with nanocomposite structures through the addition of vinyl functionalised silica nanoparticles (VSNPs) can enhance the compressive strength of the gels. *Fu et al.* developed nanocomposite PAMPS/PAAm DNHGs with varying sizes of 300 nm and 150 nm VSNPs at 1 wt % of the gel.[25] These DNHGs showed an improvement by a factor of two in fracture stress when VSNPs were crosslinked into the first network, as opposed to being used as fillers (i.e. not vinyl functionalised, and do not crosslink). There was no marked improvement in fracture strain. Recent studies show that nanoparticles in the range 80-250 nm are internalised into cells, such as stem cells, but in concentrations below 250 μg ml^{-1}, no toxicity was observed and the nanoparticles biodegraded more rapidly inside the cells than outside [26, 27]. Here, we explore the combination effect of GOx on the physical properties of the DNHGs with the addition of a nanocomposite structure.

Another objective was to refine the choice of photoinitiator. Previously, for open vessel FRP of PAAm, only 24% conversion was achieved using 1 wt% of initiator 2, 2-dimethoxy-2-pheyl acetophenone (DMPA) in the presence of GOx, which was only a 2% increase in conversion compared to the control without GOx.[10] The GOx was a mediator for redox initiation polymerizations based on the by-product hydrogen peroxide forming hydroxyl radicals[28, 29],not as a means for degassing O_2 in open vessel FRP. The initiator also caused significant loss of

cell viability at 0.05 w/v % (0.5 wt %) of DMPA and higher .[30] So, the objective here was to use Irgacure-2959, an α-cleavage photoinitiator[31, 32] that only exhibits cell toxicity at 0.1 wt/v % (1 wt %).[33, 34 30] and to investigate the combination of Irgacure-2959 and GOx, to ensure we optimize the polymerization to utilize the lowest amount of PI that results in 100 % polymer conversion.

To the best of our knowledge, GOx has not been used to create an improved system for hydrogel or DNHG synthesis for biomedical applications. In particular, this methodology allows for optimized conditions with non-cytotoxic concentrations of photoinitiator. We also extended the process to produce nanocomposite gels. This provides a dynamic alternative for open-system synthesis allowing for the fabrication of materials of specific size and shape fit for their purpose of use.

Materials and Methods

Reagents were purchased from Sigma-Aldrich (Dorset, UK) and used as received, unless stated otherwise: acrylamide (AAm; ≥99%) and 2-acrylamido-2-methyl-1-propanesulfonic acid (AMPS; 99%); N, N-methylenebis(acrylamide) (BIS; 99%); photoinitiator 2-hydroxy-4′ -(2-hydroxyethoxy)-2-methylpropiophenone (synonym Irgacure 2959; 98%), 1, 3, 5 –trioxane (≥99%); deuterium oxide (D_2O; 99.9 atom % D); ammonium hydroxide (NH_4OH; 28-30 % NH_3 basis), tetraethyl orthosilicate (TEOS, 98 %); ethanol (EtOH; 200 proof, anhydrous; ≥ 99.5 %); triethoxyvinylsilane (VTEOS; 97 %); D-glucose (G) and glucose oxidase (GOx; from aspergillus niger as a lyophilized powder) stored in phosphate buffer saline (PBS) aliquots at -20 °C. ATDC5 murine chondrogenic cell line (ATCC. UK) was used at purchased for cell

View Article Online
DOI: 10.1039/C9TB00658C

cytotoxicity studies. GOx and G were dissolved in PBS upon arrival and stored separately in aliquots of 30 µL at -20 °C to avoid freeze-thaw cycles of the enzyme and sugar. Final concentrations of GOx and D-glucose were 200 nM and 100 mM, respectively, for adding to photopolymer solutions.

Polymer synthesis

All photopolymerizations took place under the same conditions in a XL-1000 UV Crosslinker with 365 nm light for 5400 s. AAm and AMPS monomers were dissolved in deionised water under stirring at room temperature with final concentrations of 1.41 M and 0.48 M respectively. Photopolymerization was carried out in open-to-ambient glass beakers for AAm and AMPS using 0.05, 0.1, 0.5, 1 and 2 wt % PI Irgacure 2959, in the presence and absence of GOx/G (200 nM of GOx and 100 nM of glucose, G). 10 mg crystals of trioxane were added to the monomer solutions to be used as a ^{1}H NMR reference for polymer conversion calculations. For the photopolymer kinetics study, ^{1}H NMR samples were taken from the solutions at time zero as a reference for the unreacted monomer solution. The chosen time points for the study were 1, 2, 5, 10, 20, 30, 40, 50, 60, 70 and 90 minutes. A single drop (approximately 50 mg) was extracted from the photopolymer solution at each time point and quickly diluted with 500 µL D_2O to stop the reaction. In the case of PAMPS, the monomer solution was highly acidic and required neutralisation before GOx was used to prevent the enzyme becoming denatured. AMPS 2.41 M was titrated from pH 0.34 to pH 7.1 using 5.03 mL of 1 M NaOH, which allowed a final AMPS monomer concentration of 0.48 M.

Cell studies

View Article Online
DOI: 10.1039/C9TB00658C

Cell seeding for viability analyses

ATDC5 cells were seeded at 3000 cells/cm^2 in 96-well multi-well tissue-culture plates and allowed to grow for 24 h in 100 μ L basal DMEM (Dulbecco's modified eagle medium) containing 5% (v/v) FCS (foetal calf serum), 1% (v/v) penicillin-streptomycin and 1× ITS (insulin-transferring-selenium) liquid supplement. Culture medium was then replaced with DMEM containing the polymer (20% v/v) with basal supplements and cultured for further 24 h. DMEM containing 20% v/v PBS was also used as a control.

Viability of cells following was determined by 3-(4,5-dimethylthiazol-2-yl)-2,5-diphenyltetrazolium bromide (MTT) metabolic activity assay. Culture medium was replaced with 1 mg/ml MTT solution. MTT solution was removed after 2 h and dimethyl sulfoxide (DMSO) was added to dissolve the formazan crystals converted by living cells. The luminescence of the resulting solutions was measured at 570 nm.

Visualisation of cell viability was achieved by LIVE/DEAD™ staining using a combination of CellTracker™ green (CTG) and ethidium homodimer-1 (EH-1). Cultured cells were washed in PBS and incubated in CTG (10 μg ml^{-1}) and EH-1 (5 μg ml^{-1}) dye working solution for 45 minutes. The dye solution was then replaced with fresh plain DMEM and incubated for further 30 minutes. Cells were washed and fixed with 4% (w/v) paraformaldehyde (PFA) for imaging under fluorescent microscopy.

Statistical analysis of cell viability was performed using Mann-Whitney U test with Bonferroni correction (n = 3). Results were deemed significant if the probability of occurrence by random chance was less than 5% (i.e. $p<0.05$).

Mechanical Testing

View Article Online
DOI: 10.1039/C9TB00658C

Mechanical testing in compression was conducted on all swollen DNHGs samples until mechanical failure of the material was achieved. The samples were compressed using a Zwick Roell z2.5 machine fitted with a load cell of 10 kN, and a strain rate of 1.5 mm min^{-1}. Due to the nature of the hydrogel, the material was physically distorted under compression in the perpendicular direction to compression. The distortion causes an increase in the cross-sectional area where force is applied; this is known as 'barrelling'. The mass that is distorted will therefore yield a larger sample-compression plate interface that generates frictional forces that resist lateral spread[35]. This ultimately results in increased compressive forces that are required to counter the additional frictional forces, resulting in inaccurate compression profiles for the samples tested. Therefore, to correct for the distortion, conventional stress and strain were converted to real stress and strain, using Equations (1 – 4) below.

$$\text{Conventional stress } \sigma_C = \frac{F}{A_0} \quad \text{Equation (1)}$$

$$\text{Conventional strain } \varepsilon_C = \frac{\Delta L}{L_0} \quad \text{Equation (2)}$$

$$\text{Real stress } \sigma_r = \sigma_c(1 + \varepsilon_C) \quad \text{Equation (3)}$$

$$\text{Real strain } \varepsilon_r = \ln(1 + \varepsilon_C) \quad \text{Equation (4)}$$

Double network hydrogel synthesis

DNHGs were synthesised in a two-step sequential photopolymerization. AMPS monomers were dissolved under stirring in deionised water, and titrated to pH 7.1 using NaOH, to a final concentration of 0.48 M. GOx/G, 0.05 wt% PI and 1 wt% BIS were then added to the solution

View Article Online
DOI: 10.1039/C9TB00658C

and stirred for 5 minutes. The solution was then poured into a 48-well multi-well polystyrene plate without being covered and placed into the XL-1000 UV Crosslinker for photopolymerization of the first network under 365 nm light for 1.5 h. Once completed, the gels were removed from the multi-well and heated at 60°C overnight for 24 h to denature GOx. The gels were then soaked in a 1.41 M concentration solution of AAm monomers with 0.5 wt% PI, 0.1 wt% BIS, and GOx/G. The swollen gels were placed back into the UV Crosslinker on glass plates for 1.5 h to form the second network. These samples are referred to as GOx controls. A control sample without GOx was synthesised next using the same method, without the addition of GOx/G. DNHGs were then dried at 60°C for 3 days.

Functionalised silica nanoparticle synthesis

Silica nanoparticles (SNPs) were synthesised using a modified Stöber process [36] using fixed molar concentrations of TEOS (0.28 M) and water (6 M), and adjusting NH_4OH to achieve diameters of 50 nm and 150 nm. 150 nm SNP were synthesized with 82.28 ml EtOH and 10.27 ml DI H_2O, to which 0.3 M NH_4OH (1.19 ml) and 6.25 ml TEOS were added. The solution was left to stir at 500 rpm for 24 h. The final milky white sol was centrifuged using an Eppendorf 5430 and washed with EtOH three times at 7,830 rpm to remove unreacted TEOS. The final precipitate was left to dry at 60 ^{o}C overnight. The 50 nm SNPs were synthesized using 0.2 M of NH_4OH.

Vinyl functionalisation was achieved by dispersing 500 mg SNPs in 10 ml EtOH and sonicating the solution using the CamSonix 1800T until it was fully dispersed. The solution was then topped up with 90 ml EtOH on a stirring plate. 500 µl NH_4OH and 3 ml VTEOS were added to the solution and left to stir for 24 h. The solution was then centrifuged and washed three times with EtOH to remove unreacted VTEOS. The final precipitate was dried at 60 ^{o}C and stored under dry conditions. VSNP results can be found in the supplementary section.

View Article Online
DOI: 10.1039/C9TB00658C

Nanocomposite gel synthesis

DNHGs containing 20 wt % of 150 nm or 50 nm VSNPs in the first network as cross linkers were synthesised using the method above, and represented in Figure 1. VSNPs were dispersed and sonicated in 1 ml deionised water and then added to the titrated solution containing AMPS monomers and GOx/G. The rest of the steps described above for DNHG synthesis were followed. All of the synthesised DNHGs were swollen in water and weighed daily until a swelling plateau was reached.

Results and Discussion

At 0.05 wt% PI, ^{1}H NMR of PAMPS showed 0 % conversion in the absence of GOx due to instant and rapid inhibition of PI radicals by O_2 (Scheme 1) , meaning that free radicals are quenched at a faster rate by O_2 than they can react with monomers [14] This confirms that O_2 inhibition cannot be overcome at the low PI concentrations needed to maintain cell viability. In contrast, 100 % conversion was achieved at the same PI concentration (0.05 wt%) in the presence of GOx (H^1 NMR spectra can be found in the supplementary section). These results prove that GOx evaded all O_2 inhibition steps in PAMPs, labelled e1, e2 and e3 in Scheme 1. Significantly, GOx at 200 nM was sufficient to eliminate the scavenging effects of O_2 despite its remarkably low concentration.[23]

Higher concentrations of PI were used to investigate the kinetics and pathways of inhibition in more detail. Table 1 shows that at 0.1 wt% PI the PAMPS control (no GOx) exhibited 35 % conversion. Increasing the PI concentration for PAMPS 20 fold, from 0.1 wt% to 2 wt% increased the conversion from 35% to 95% (Figure 2a). This increase agrees with the concept

of overcoming the scavenging effects of O_2 in FRP by increasing PI concentration, but at a cost. PI concentrations above 0.1 wt% are not favoured in biomaterial applications due to their potential cytotoxic effects,[37] and using 20 times the concentration of PI still did not provide 100 % conversion. Furthermore, PI solubility is reduced significantly at 2 wt% and can reduce optical clarity, hindering the UV light interaction.

Figure 2b shows that PAAm control conversions exhibited a near linear relationship with increasing PI concentration. Higher PI concentrations of 1 wt% were needed to reach 100 % conversion in the presence of GOx for PAAm, compared to the 0.05 wt% PI for PAMPS. Without GOx, the control PAAm only reached 40 % conversion (Figure 2b) at 1 wt% PI and was below 80 % at 2 wt% PI. ^{1}H NMR graphs showing polymer conversion of PAMPS and PAAm can be found in the supplementary information. The viscosity and appearance of control PAAm the solution was wet, sticky and inconsistent. This is a consequence of the apparent long inhibition times caused by a lack of initiating radicals that are scavenged rapidly by O_2. [13, 38] In contrast, PAAm formed with GOx exhibited gel-like texture.

The efficacy of GOx was better for PAMPS than PAAm, suggesting that PAAm is more sensitive to O_2 and exhibits slower reaction kinetics. Figure 3a shows the kinetic profile of PAMPS at 0.5 wt% PI drastically improved in the presence of GOx, achieving 100 % conversion in less than 30 minutes. In contrast, the control shows a lag of 30 minutes before the polymers began to form. PAAm kinetics follows a similar trend for the control, and improved kinetics with GOx reaching full conversion in less than 70 minutes. The improved reaction rate with GOx and low PI concentrations can have extremely useful implications for soft material synthesis such as hydrogels and processing materials containing cells, including bioprinting.

View Article Online
DOI: 10.1039/C9TB00658C

Figure 4 demonstrates the change in visible viscosity of the polymer solutions at 90 minutes. PAAm produced with GOx became gel-like, whilst the control exhibited inconsistent and wet texture due to its incomplete polymerization. Polymers containing GOx changed colour from clear to yellow approximately 24 h post photopolymerization. This observation suggests that GOx continues degassing the system for up to 24 h. This gives an indication that 200 nM of GOx could be a sufficient value for polymerizations that last up to 24 h.

Cytotoxicity studies using ATDC5 cells were carried out in media containing PAAm and PAMPS made with varying PI concentrations in the presence of GOx. PAAm and PAMPS controls (without GOx) were synthesized using 0.5 wt% PI. Results of the cytotoxicity studies were compared to DMEM and DMEM/PBS (20% v/v) only controls. Chondrocytes were seeded at 0 h post synthesis, 24 h post synthesis and 24 h post synthesis following an additional 60 °C heat treatment. The LIVE/DEAD™ assay in Figure 5Figure 4 shows low cell survival for PAAm control at 0 h post synthesis and after 24 h at room temperature, and after 24 h at 60 °C, due to unreacted monomers in the solution that are toxic. Cell survival was expected to increase in the presence of GOx because of the 100% conversion of the toxic monomers; however cell survival only increased for PAAm in the presence of GOx when the gel was heated to 60 °C 24 h post synthesis (Figure 6). The cell death occurring when the gels were not heated was attributed to cell asphyxiation due to the effective nature of GOx. Cell survival increased once the enzyme was denatured at 60 °C, and any cell death exhibited at that point was due to unreacted monomers. An asterisk represents a significant difference between cell survival for samples with GOx and control.

The MTT assay was performed in accordance with ISO 10993-5 and 10993-12 to evaluate the cytotoxicity of the polymers. Under ISO 10993, a reduction of cell viability exceeding 30 % in comparison with non-toxic controls is considered cytotoxic.[39, 40]

View Article Online
DOI: 10.1039/C9TB00658C

When the PI concentration was increased, and gels were heated to 60 °C, cell survival increased further, reaching 84% of the DMEM positive control at 0.5 wt% PI (Figure 6). The plus symbol represents a significant different between samples of ≥ 0.5 wt% PI with GOx, compared to PI of 0.05 wt % and 0.1 wt % with GOx, and control.

Figure 7 and Figure 8 show PAMPS control was non-cytotoxic, suggesting that any remaining monomers are not toxic. PAMPS is usually toxic due to its highly acidic nature however it was neutralized prior to use. Cell death for PAMPS in the presence of GOx (Figure 8) was attributed to oxygen depletion in the presence of active GOx in the gels that were not heated. High cell survival was observed for PAMPS once GOx was denatured at 60 °C. An asterisk is used to represent a significant difference between cell survivals of samples with GOx after heat treatment in comparison to 0 h and 24 h samples with GOx at room temperature.

Ultimately, denaturing GOx is essential for cell survival post gel production as the enzyme is still active. This provides clearer proof that the enzyme is suitable for polymerizations that have longer kinetics that also require an oxygen free atmosphere. Lower concentrations of GOx can be used effectively for shorter polymerizations.

Figure 9 shows the final product of the double network hydrogel formed in the presence of GOx, before and after swelling in water for 4 days. When fully swollen, the content of the hydrogel was 95% water, and its volume increased by 825%. The swelling ability of the gel, as well as its mechanical properties, can be tailored based different concentrations of cross linker used in both the 1st and 2nd network.

SEM images of control DNHG (

Figure 10 a, b) show typical porous structures of freeze dried hydrogels, throughout the material. Cross section SEM images of DNHGs containing 150 nm VSNPs synthesised in the presence of GOx (

View Article Online
DOI: 10.1039/C9TB00658C

Figure 10 c, d) reveal that VSNPs were distributed within the walls of the material. This suggests that the VSNPs (indicated with white arrows) are well integrated into the DNHGs. Polymer chains that are cross linked to VSNPs within the DNHG walls are expected to provide extra resistance against stress, providing the material with enhanced mechanical properties.

Mechanical testing was conducted on DNHG controls in the presence and absence of GOx, and on DNHGs containing 50 nm and 150 nm VSNPs in the first network (

Figure 11). Controls in the absence of GOx exhibited a compressive fracture stress of 0.10 ± 0.06 MPa with fracture strain of 45.88 ± 2.13 %. The addition of GOx to the control generated a significant increase in compressive fracture stress. The results showed that the fracture compressive stress could be increased by approximately 10 x through the addition of GOx, achieving 0.99 ± 0.24 MPa with a fracture strain of 50.15 ± 6.34 %. These excellent enhancements were attributed to the increased efficiency in the polymerization steps of the first and second networks solely due to the addition of GOx, leading to better integration within the double network structure. These results are summarised in Table 2. This, therefore, improves the synergetic effect of both networks leading to improved mechanical properties. Additionally, the integration of VSNPs, in the presence of GOx, in the first network demonstrated a further improvement in mechanical properties in both stress and strain. DNHGs containing 150 nm VSNPs with 20 wt % loading resulted in compressive fracture stress of 2.62 ± 0.48 MPa and fracture strain of 53.23 ± 4.14 %. DNHGs containing 50 nm VSNPs at 20 wt % loading resulted in compressive fracture stress 3.55 ± 0.41 MPa and fracture strain of 55.36 ± 4.06 %. The smaller VSNPs have a larger specific surface area for cross linking and polymer interaction, providing the hydrogel with improved mechanical properties relative to samples using 150 nm VSNPs. These results provide a starting point for tailoring DNHGs for different applications based on mechanical properties.

The removal of O_2 from the reaction system provides 100 % polymer conversion, resulting in a higher density of polymers in the hydrogels. This leads to a higher density of cross linked polymers that can interact with VSNPs, as well as better polymer entanglement, resulting in the improved properties of the DNHGs. The addition of GOx and VSNPs improved the materials properties in both compressive stress and strain. Ultimately, ensuring an oxygen free atmosphere through the addition of GOx can play a vital role in achieving enhanced mechanical properties for DNHGs to be similar to that of native articular cartilage.

Conclusion

PAAm and PAMPS polymers were successfully synthesized through open vessel FRP at 100% conversion with faster and improved kinetics in the presence of GOx compared to previous studies. These results were achieved using Irgacure-2959 (photoinitiator) concentrations that have been reported as non-cytotoxic, and the resulting polymers were not cytotoxic once GOx was denatured. Double network hydrogels were successfully made in the presence of GOx, and their mechanical properties increased significantly with the addition of GOx. Further improvements were achieved by the addition of functionalized silica nanoparticles as cross linkers. The combination of an O_2 atmosphere and nanocomposite cross linkers provided a tailored and enhanced biomaterial. This versatile method is a gateway to synthesizing polymeric materials such as double network hydrogels and other biomaterials in ambient vessels using non-cytotoxic photoinitiator concentrations.

View Article Online
DOI: 10.1039/C9TB00658C

Acknowledgements

This work is supported by Qatar Foundation and EPSRC grant (EP/I020861/1). The authors of this work are grateful to Dr Robert Chapman for his initial suggestions with this work. Raw data can be obtained on request from rdm-enquiries@imperial.ac.uk.

Author Information

Corresponding Author

*E-mail: julian.r.jones@imperial.ac.uk.

Author Contributions

The manuscript was written with contributions with all authors. All experiments were carried out by Dr Ali Mohammad. Dr Justin J Chung and Mr. Juan A. Milan assisted with polymer kinetics and Dr Siwei Li performed cell studies. All authors have given approval to the final version of the manuscript.

References

1. K. T. Nguyen and J. L. West, *Biomaterials*, 2002, **23**, 4307-4314.
2. J. Jagur-Grodzinski, *Polymers for Advanced Technologies*, 2006, **17**, 395-418.
3. G. Vunjak-Novakovic, B. Obradovic, I. Martin, P. M. Bursac, R. Langer and L. E. Freed, *Biotechnology Progress*, 1998, **14**, 193-202.
4. J. A. Hubbell, *Nat Biotech*, 1995, **13**, 565-576.
5. M. A. Haque, T. Kurokawa and J. P. Gong, *Polymer*, 2012, **53**, 1805-1822.
6. J. P. Gong, Y. Katsuyama, T. Kurokawa and Y. Osada, *Adv Mater*, 2003, **15**.
7. S. Liang, Q. M. Yu, H. Yin, Z. L. Wu, T. Kurokawa and J. P. Gong, *Chemical Communications*, 2009, DOI: 10.1039/B916581A, 7518-7520.
8. W. Yang, H. Furukawa and J. P. Gong, *Advanced Materials*, 2008, **20**, 4499-4503.
9. J. Hu, K. Hiwatashi, T. Kurokawa, S. M. Liang, Z. L. Wu and J. P. Gong, *Macromolecules*, 2011, **44**, 7775-7781.
10. F. Oytun, M. U. Kahveci and Y. Yagci, *Journal of Polymer Science Part A: Polymer Chemistry*, 2013, **51**, 1685-1689.
11. P. Barto, in *Stereolithography*, ed. P. J. Bártolo, Springer US, 2011, vol. 1, ch. 7, pp. 169-170.
12. K. Studer, C. Decker, E. Beck and R. Schwalm, *Progress in Organic Coatings*, 2003, **48**, 92-100.
13. Y. Yagci, S. Jockusch and N. J. Turro, *Macromolecules*, 2010, **43**, 6245-6260.
14. J.-P. Fouassier, in *Photoinitiation, Photopolymerization, and Photocuring: Fundamentals and Applications*, ed. J.-P. Fouassier, Hanser Gardner Publications, 1995-01, vol. 1, ch. 5, p. 199.
15. F. R. Wight, *Journal of Polymer Science: Polymer Letters Edition*, 1978, **16**, 121-127.
16. C. Decker and A. D. Jenkins, *Macromolecules*, 1985, **18**, 1241-1244.
17. A. K. O'Brien and C. N. Bowman, *Macromolecules*, 2006, **39**, 2501-2506.
18. C. Belon, X. Allonas, C. Croutxé-barghorn and J. Lalevée, *Journal of Polymer Science Part A: Polymer Chemistry*, 2010, **48**, 2462-2469.
19. E. Andrzejewska, *Progress in Polymer Science*, 2001, **26**, 605-665.
20. S. Inbar, H. Linschitz and S. G. Cohen, *Journal of the American Chemical Society*, 1982, **104**, 1679-1682.
21. R. F. Bartholomew and R. S. Davidson, *Journal of the Chemical Society C: Organic*, 1971, DOI: 10.1039/J39710002342, 2342-2346.
22. D. K. Balta, N. Arsu, Y. Yagci, S. Jockusch and N. J. Turro, *Macromolecules*, 2007, **40**, 4138-4141.
23. R. Chapman, A. J. Gormley, K.-L. Herpoldt and M. M. Stevens, *Macromolecules*, 2014, **47**, 8541-8547.
24. A. J. Gormley, R. Chapman and M. M. Stevens, *Nano Letters*, 2014, **14**, 6368-6373.
25. Q. Wang, R. Hou, Y. Cheng and J. Fu, *Soft Matter*, 2012, **8**, 6048-6056.
26. P. Naruphontjiralcul, A. E. Porter and J. R. Jones, *Acta Biomater*, 2018, **66**, 67-80.
27. O. Tsigkou, S. Labbaf, M. M. Stevens, A. E. Porter and J. R. Jones, *Adv. Healthc. Mater.*, 2014, **3**, 115-125.
28. R. Shenoy and C. N. Bowman, *Biomaterials*, 2012, **33**, 6909-6914.
29. B. J. Berron, L. M. Johnson, X. Ba, J. D. McCall, N. J. Alvey, K. S. Anseth and C. N. Bowman, *Biotechnology and Bioengineering*, 2011, **108**, 1521-1528.
30. L. Xu, N. Sheybani, W. A. Yeudall and H. Yang, *Biomaterials science*, 2015, **3**, 250-255.
31. D. R. Albrecht, V. L. Tsang, R. L. Sah and S. N. Bhatia, *Lab on a Chip*, 2005, **5**, 111-118.

32. J. Baier Leach, K. A. Bivens, C. W. Patrick Jr and C. E. Schmidt, *Biotechnology and Bioengineering*, 2003, **82**, 578-589.
33. C. G. Williams, A. N. Malik, T. K. Kim, P. N. Manson and J. H. Elisseeff, *Biomaterials*, 2005, **26**, 1211-1218.
34. S. J. Bryant, C. R. Nuttelman and K. S. Anseth, *Journal of Biomaterials Science, Polymer Edition*, 2000, **11**, 439-457.
35. M. Jerabek, Z. Major and R. W. Lang, *Polymer Testing*, 2010, **29**, 302-309.
36. W. Stöber, A. Fink and E. Bohn, *Journal of Colloid and Interface Science*, 1968, **26**, 62-69.
37. A. Sabnis, M. Rahimi, C. Chapman and K. T. Nguyen, *Journal of Biomedical Materials Research Part A*, 2009, **91A**, 52-59.
38. A. D. Jenkins, *Polymer International*, 2000, **49**, 1729-1729.
39. ISO, 2009, **10993-5:2009**, 34.
40. ISO, 2012, **10993-12:2012**, 20.

Tables

Table 1. PAAm and PAMPS conversion for control and in the presence of 200 nM GOx for different photoinitiator (PI) concentrations.

	PAMPS Conversion (%)		PAAm Conversion (%)	
PI wt%	Control	GOx	Control	GOx
0.05	0	100	0	78
0.1	35	100	4	92
0.5	59	100	17	98
1	76	100	40	100
2	95	100	76	100

Table 2 - Summary of mechanical tests of DNHGs showing compressive strength (MPa) and fracture strain (%) of control (no VSNPs or GOx), GOx control (made with GOx but not VSNPs), DNHGs loaded with 20 wt % VSNPs of 150 nm and 50 nm.

			Loading with 20 wt % VSNPs	
	Control	GOx Control	150 nm	50 nm
Fracture Compressive Stress (MPa)	0.10 ± 0.06	0.99 ± 0.24	2.62 ± 0.48	3.55 ± 0.41
Fracture Strain %	45.88 ± 2.13	50.15 ± 6.34	53.23 ± 4.14	55.36 ± 4.05

Captions

Scheme 1. The oxygen inhibition (i1–i3) and evasion (e1–e3) pathway in photopolymerization [10-13].

Figure 1. Schematic representation showing the synthesis route for nanocomposite PAMPS/ PAAm double network hydrogels (DNHG).

Figure 2. Conversion profiles for polymers with increasing wt% PI with GOx and controls (without GOx) at 90 minutes for a) PAMPS and b) PAAm.

Figure 3. Kinetics of the control reactions and in the presence of GOx at for a) PAMPS at 0.5 wt% PI and b) PAAm at 1 wt% PI.

Figure 4. Photographs of a) PAMPS and b) PAAm solutions at 90 minutes; using 0.1 wt% PI in the presence and absence of GOx.

Figure 5. LIVE/DEAD™ cell viability assay for ATDC5 cells cultured in DMEM containing PAAm that was polymerized in the presence of 200 nM of GOx at varying PI concentrations and heated for 24 h at room temperature or 60°C. Scale bar is 50 μm for all figures.

Figure 6. Cell viability for ATDC5 cells in DMEM with 20 wt% PAAm that was polymerized in the presence of 200 nM GOx at varying PI concentrations and control (C) at 0.5 wt% PI and heated for 24 h at room temperature or 60°C; * $p<0.05$ compared to 0 h and 24 h (room temperature). + $p<0.05$ compared to control (0.5 wt % PI, GOx 0.05 wt % PI and GOx 0.1 wt % PI).

Figure 7. LIVE/DEAD™ cell viability assay for ATDC5 cells cultured in DMEM containing PAMPS that was polymerized in the presence of 200 nM of GOx at varying PI concentrations and heated for 24 h at room temperature or 60°C before. Scalebar is 50 μm for all figures.

Figure 8. Cell viability for ATDC5 cells in DMEM with 20 wt% PAMPS that was polymerized in the presence of 200 nM of GOx at varying PI concentrations and heated for 24 h at room temperature or 60 °C; * $p<0.05$ compared to 0 h and 24 h (room temperature).

View Article Online
DOI: 10.1039/C9TB00658C

Figure 9. Double network PAMPS/PAAm hydrogels (0.05 wt% PI) formed in the presence of 200 nM GOx (and aged at 60 °C for 24 h), as produced form (left) and after swelling in water for 4 days in water.

Figure 10. SEM images of (a, b) control PAMPS/PAAm DNHGs ((a) scalebar is 50 μm, (b) scalebar is 20 μm), and (c, d) PAMPS/PAAm DNHG containing 150 nm VSNPs synthesised in the presence of GOx ((c) scalebar is 2 μm, (d) scalebar is 1 μm). White arrows are inserted to highlight the VSNPs within the DNHG.

Figure 11. Compression curves for PAMPS/PAAm DNHGs (10 mm x 15 mm) containing 150 nm and 50 nm vinyl functionalized silica nanoparticles (VSNPs) at 20 wt % loading, compared to a control (no VSNPs or GOx), and a control containing GOx but no VSNPs. TEM images of VSNPs with diameter 150 nm with scalebar 0.2 μm (left) and 50 nm with scalebar 2 μm (right) have been added on the graph.

View Article Online
DOI: 10.1039/C9TB00658C

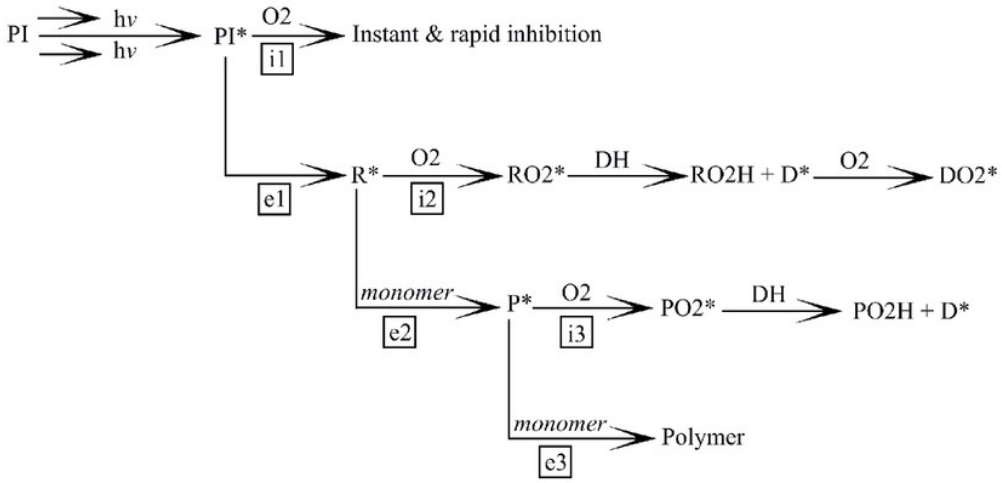

Scheme 1. The oxygen inhibition (i1–i3) and evasion (e1–e3) pathway in photopolymerization 10-13.

69x33mm (300 x 300 DPI)

View Article Online
DOI: 10.1039/C9TB00658C

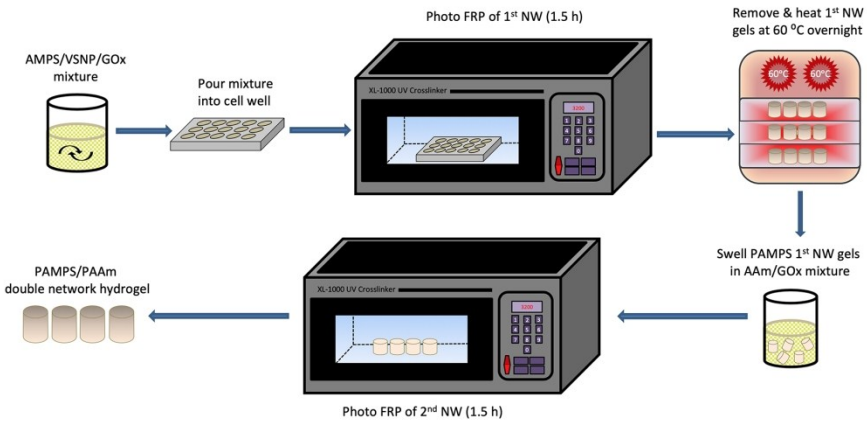

Figure 1. Schematic representation showing the synthesis route for nanocomposite PAMPS/ PAAm double network hydrogels (DNHG).

View Article Online
DOI: 10.1039/C9TB00658C

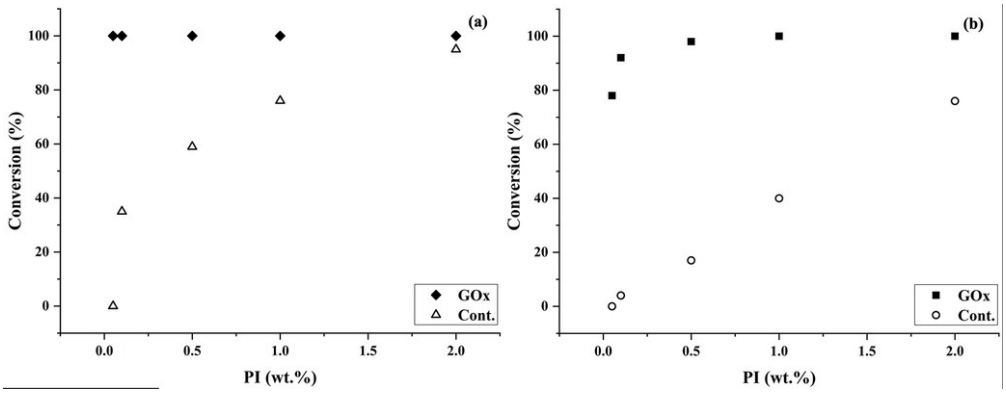

Figure 2. Conversion profiles for polymers with increasing wt% PI with GOx and controls (without GOx) at 90 minutes for a) PAMPS and b) PAAm.

87x33mm (300 x 300 DPI)

View Article Online
DOI: 10.1039/C9TB00658C

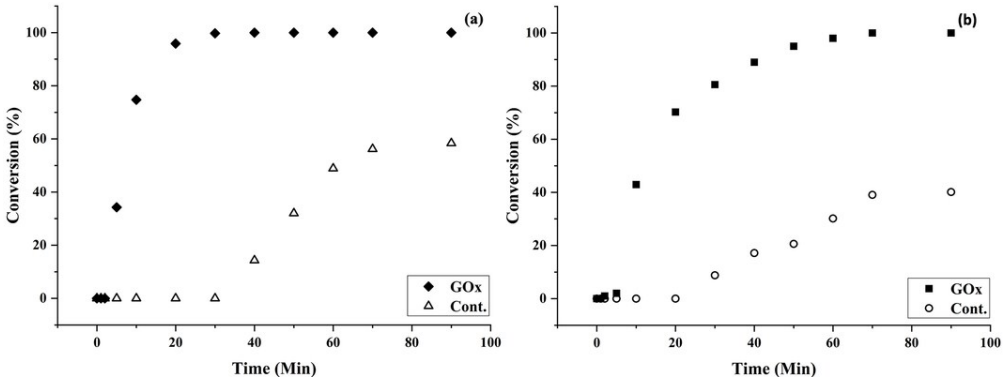

Figure 3. Kinetics of the control reactions and in the presence of GOx at for a) PAMPS at 0.5 wt% PI and b) PAAm at 1 wt% PI.

90x33mm (300 x 300 DPI)

View Article Online
DOI: 10.1039/C9TB00658C

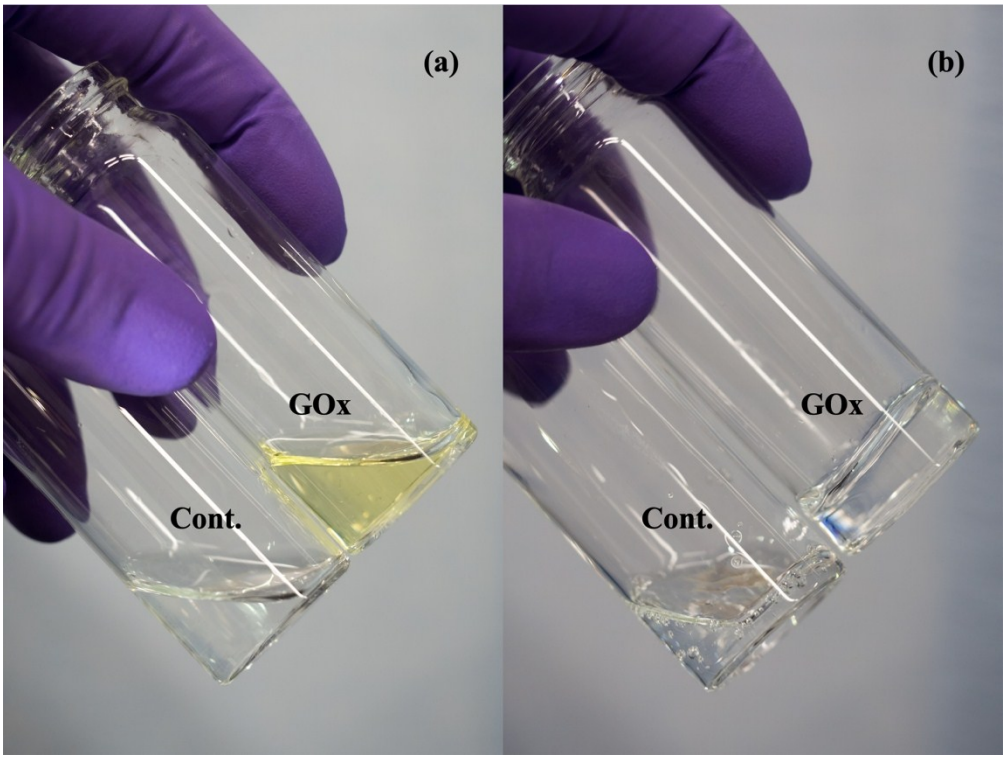

Figure 4. Photographs of a) PAMPS and b) PAAm solutions at 90 minutes; using 0.1 wt% PI in the presence and absence of GOx.

View Article Online
DOI: 10.1039/C9TB00658C

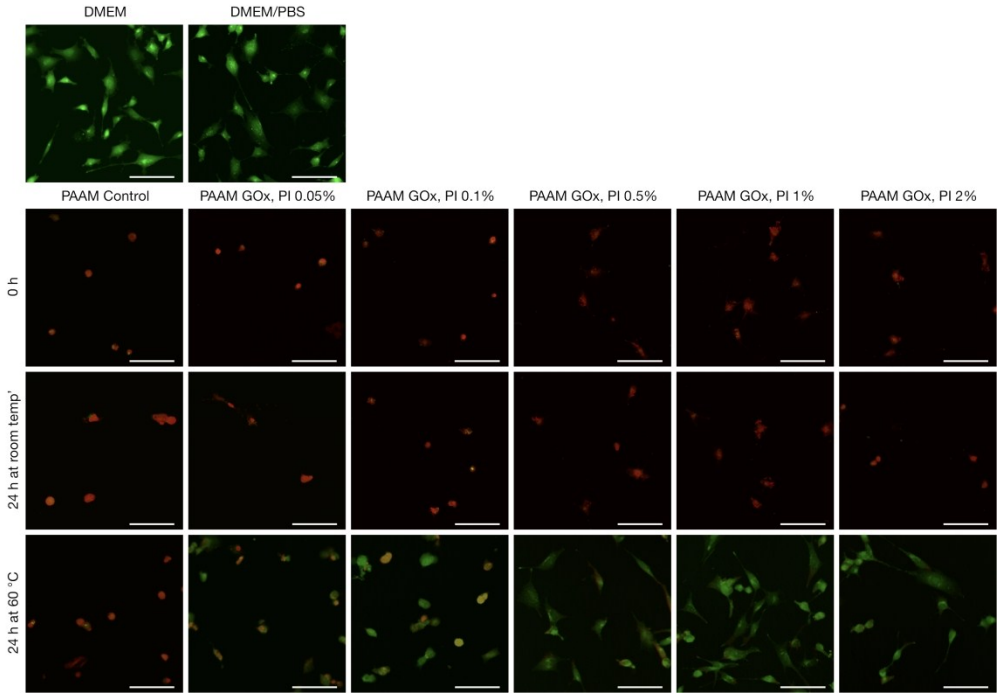

Figure 5. LIVE/DEADTM cell viability assay for ATDC5 cells cultured in DMEM containing PAAm that was polymerized in the presence of 200 nM of GOx at varying PI concentrations and heated for 24 h at room temperature or 60□C. Scale bar is 50 μm for all figures.

241x167mm (300 x 300 DPI)

View Article Online
DOI: 10.1039/C9TB00658C

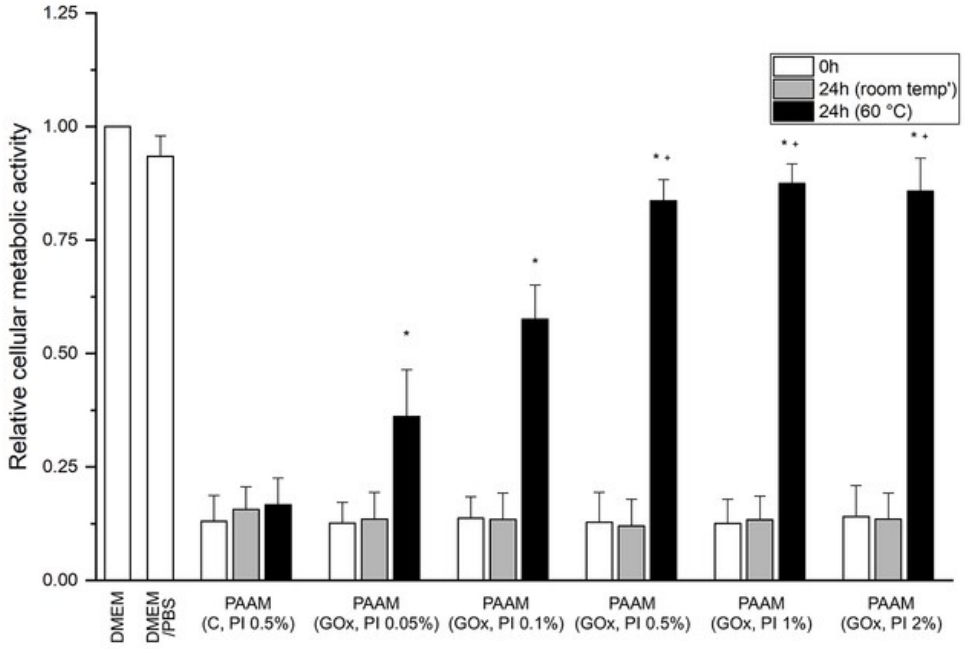

Figure 6. Cell viability for ATDC5 cells in DMEM with 20 wt% PAAm that was polymerized in the presence of 200 nM GOx at varying PI concentrations and control (C) at 0.5 wt% PI and heated for 24 h at room temperature or 60□C; * p<0.05 compared to 0 h and 24 h (room temperature). + p<0.05 compared to control (0.5 wt % PI, GOx 0.05 wt % PI and GOx 0.1 wt % PI).

55x42mm (300 x 300 DPI)

View Article Online
DOI: 10.1039/C9TB00658C

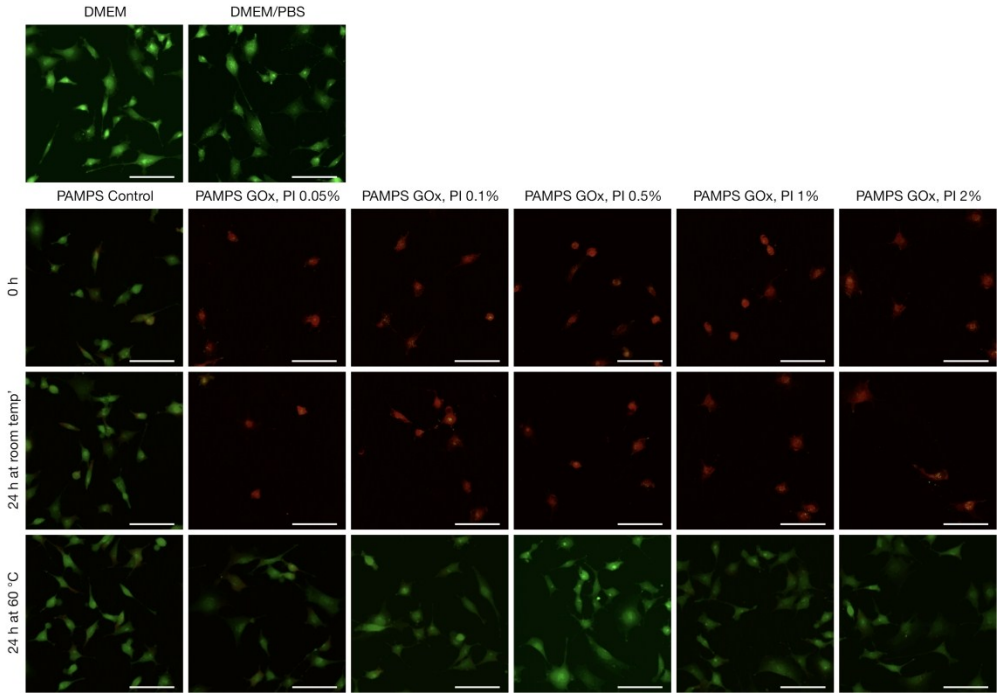

Figure 7. LIVE/DEADTM cell viability assay for ATDC5 cells cultured in DMEM containing PAMPS that was polymerized in the presence of 200 nM of GOx at varying PI concentrations and heated for 24 h at room temperature or 60□C before. Scalebar is 50 μm for all figures.

241x167mm (300 x 300 DPI)

View Article Online
DOI: 10.1039/C9TB00658C

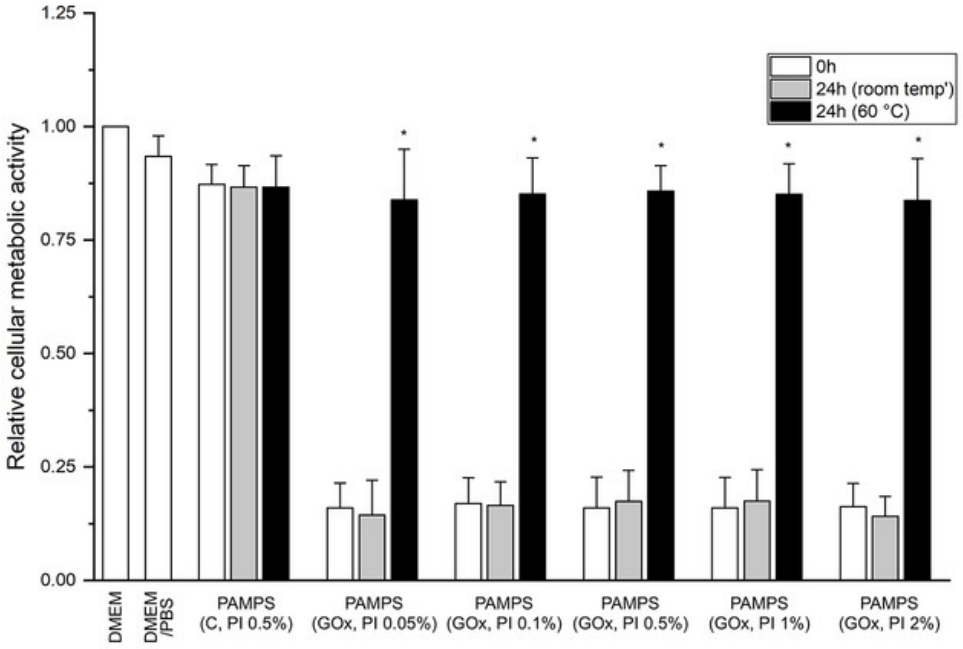

Figure 8. Cell viability for ATDC5 cells in DMEM with 20 wt% PAMPS that was polymerized in the presence of 200 nM of GOx at varying PI concentrations and heated for 24 h at room temperature or 60 ☐C; * $p<0.05$ compared to 0 h and 24 h (room temperature).

55x42mm (300 x 300 DPI)

View Article Online
DOI: 10.1039/C9TB00658C

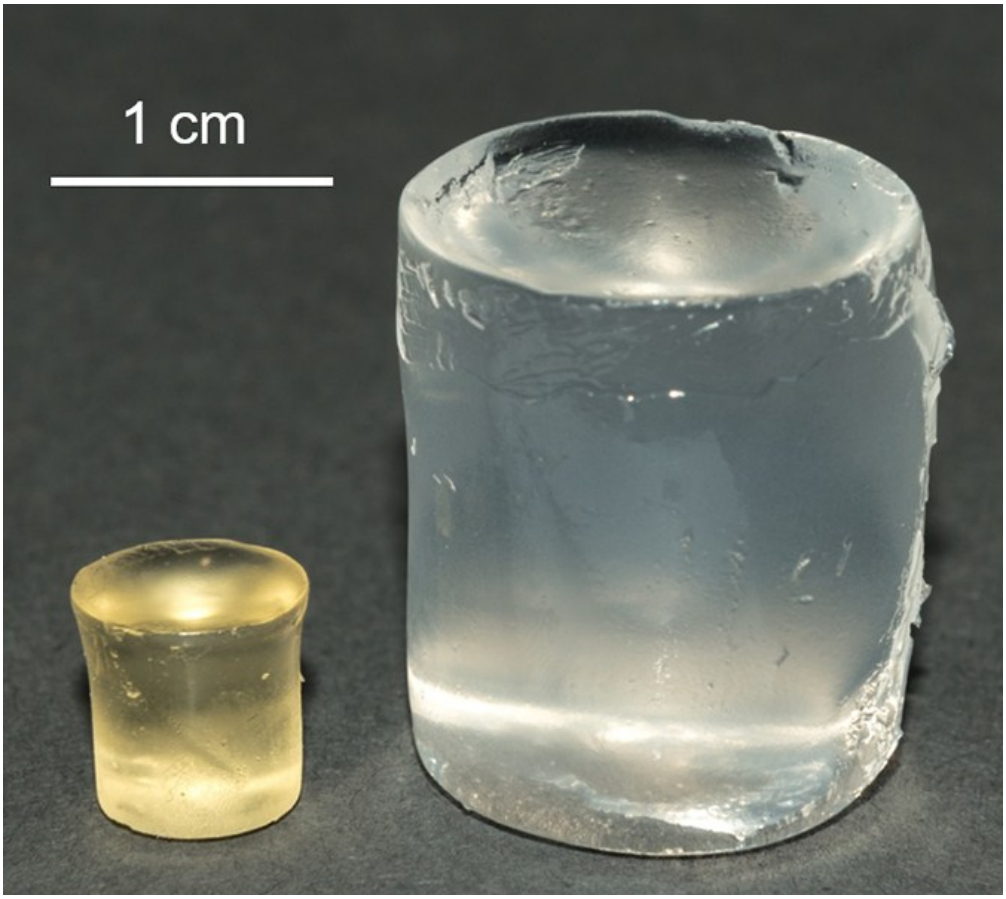

Figure 9. Double network PAMPS/PAAm hydrogels (0.05 wt% PI) formed in the presence of 200 nM GOx (and aged at 60 ☐C for 24 h), as produced form (left) and after swelling in water for 4 days in water.

View Article Online
DOI: 10.1039/C9TB00658C

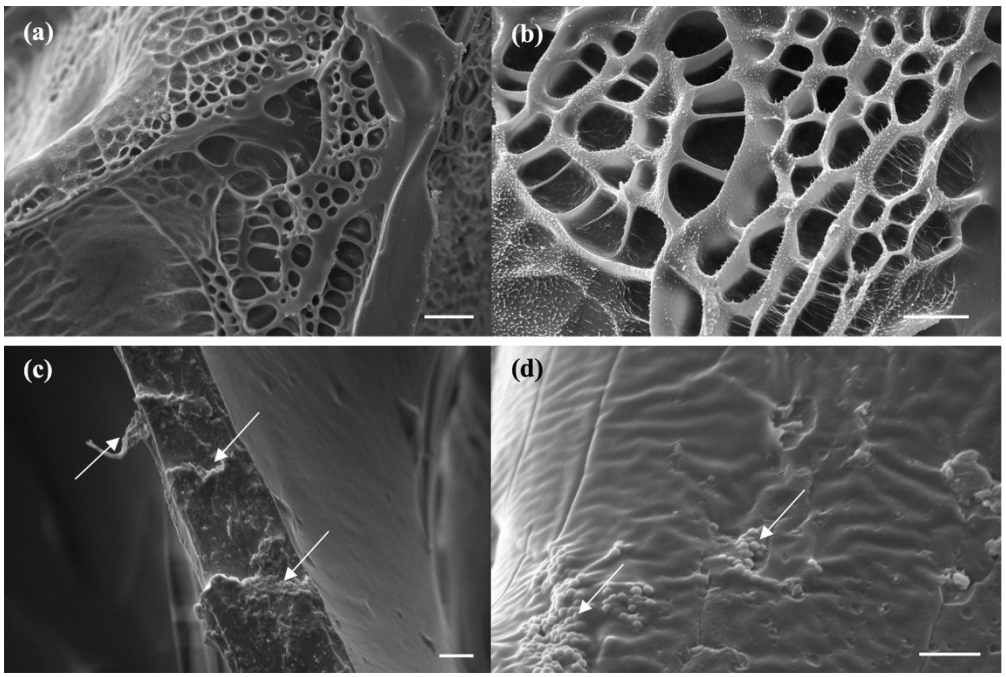

Figure 10. SEM images of (a, b) control PAMPS/PAAm DNHGs ((a) scalebar is 50 μm, (b) scalebar is 20 μm), and (c, d) PAMPS/PAAm DNHG containing 150 nm VSNPs synthesised in the presence of GOx ((c) scalebar is 2 μm, (d) scalebar is 1 μm). White arrows are inserted to highlight the VSNPs within the DNHG.

View Article Online
DOI: 10.1039/C9TB00658C

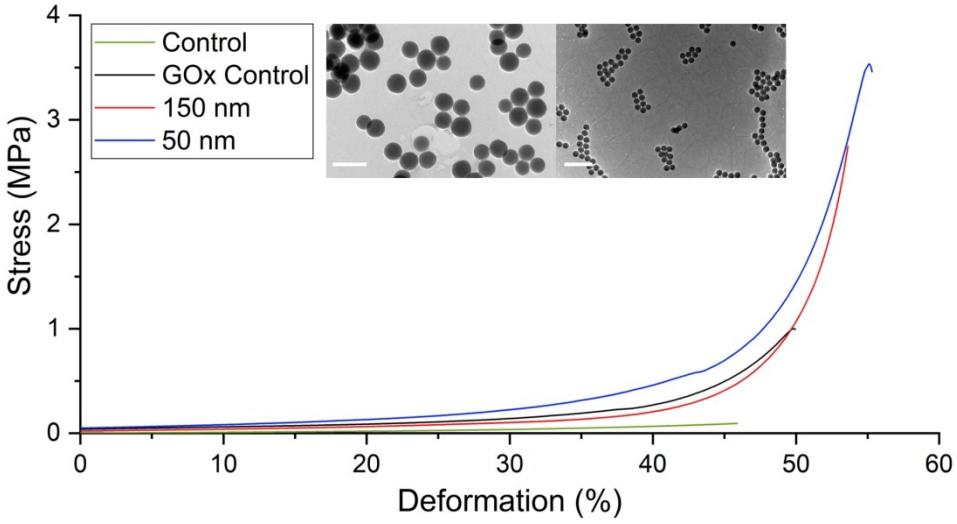

Figure 11. Compression curves for PAMPS/PAAm DNHGs (10 mm x 15 mm) containing 150 nm and 50 nm vinyl functionalized silica nanoparticles (VSNPs) at 20 wt % loading, compared to a control (no VSNPs or GOx), and a control containing GOx but no VSNPs. TEM images of VSNPs with diameter 150 nm with scalebar 0.2 μm (left) and 50 nm with scalebar 2 μm (right) have been added on the graph.